Since January 2020 Elsevier has created a COVID-19 resource centre with free information in English and Mandarin on the novel coronavirus COVID-19. The COVID-19 resource centre is hosted on Elsevier Connect, the company's public news and information website.

International Journal of Biological Macromolecules 229 (2023) 413–421

Contents lists available at ScienceDirect

International Journal of Biological Macromolecules

journal homepage: www.elsevier.com/locate/ijbiomac

Inhibitory effects of fucoidan from *Laminaria japonica* against some pathogenic bacteria and SARS-CoV-2 depend on its large molecular weight

Xiaona Sun [a], Chunqing Ai [a,b], Chengrong Wen [a,b], Haoran Peng [c], Jingfeng Yang [a,b], Yuna Cui [a], Shuang Song [a,b,*]

[a] School of Food Science and Technology, National Engineering Research Center of Seafood, Dalian Polytechnic University, Dalian 116034, PR China
[b] National & Local Joint Engineering Laboratory for Marine Bioactive Polysaccharide Development and Application, Dalian Polytechnic University, Dalian 116034, PR China
[c] Department of Biomedical Defense, Faculty of Naval Medicine, Naval Medical University (Second Military Medical University), Shanghai 200433, PR China

ARTICLE INFO

Keywords:
Sulfated polysaccharide
Foodborne pathogen
Virus
Photocatalytic degradation

ABSTRACT

Fucoidan is a highly sulfated polysaccharide with a wide range of bioactivities, including anti-pathogenic activity. However, the relationship between structure and activity of fucoidan in inhibiting pathogen infections remains unclear. Here, different-molecular-weight fucoidans were prepared by photocatalytic degradation followed by membrane ultrafiltration, and their chemical structures and anti-pathogenic microbiota activity were compared. Results showed that photocatalytic degradation could effectively degrade fucoidan while its structure block and sulfate groups were not destroyed obviously. Fucoidan (90.8 kDa) of 5 mg/mL could inhibit the growth of *S. aureus*, *S. typhimurium* and *E. coli*, but its degradation products, Dfuc1 (19.2 kDa) and Dfuc2 (5.5 kDa), demonstrated lower inhibitory effect. In addition, compared to Dfuc1 and Dfuc2, fucoidan showed stronger capability to prevent the adhesion of *S. aureus*, *L. monocytogenes*, *V. parahaemolyticus* and *S. typhimurium* to HT-29 cells. Moreover, the inhibitory effect against SARS-CoV-2 and the binding activity to S protein were also positively correlated to molecular weight. These results indicate that natural fucoidan with higher molecular weight are more effective to inhibit these pathogenic bacteria and SARS-CoV-2, providing a better understanding of the relationship between structure and activity of fucoidan against pathogenic microbiota.

1. Introduction

Fucoidan is an edible highly sulfated polysaccharide that mainly exists in brown algae, e.g. *Laminaria japonica*, *Undaria pinnatifida*, *Sargassum muticum*, and commonly isolated by hot water extraction [1], acid extraction [2], enzymolysis extraction method [3]., etc. Typically, fucoidan has a backbone of α-(1,3) linked L-fucose residues or alternating repeating units of α-(1,3) and α-(1,4)-linked L-fucose residues with variable degrees of sulphation [4]. It is mainly comprised of L-fucose and sulfate groups, together with small amounts of glucose, galactose, mannose and uronic acid, which vary depending on algae species, harvesting season, and purification process [5]. At present, fucoidan and their low molecular weight derivatives exhibit a variety of biological activities, including anti-cancer [6], anti-coagulation [7], anti-thrombus [8], anti-oxidation [9] and anti-virus [10], and have already been commercialized as functional food ingredients, dietary supplements or cosmetology products because of their health-promoting activities and relatively low toxicity. [8–11].

According to previous studies, the biological activities of fucoidan depend strongly on their structural properties, especially molecular weight [12]. Recently, some studies have shown that the anti-pathogenic activity of fucoidan was increased with the reduction of molecular weight [13]. Krylova et al. [14] reported that depolymerized fucoidan (~6KDa) from *Fucus evanescens* fraction displayed a greater antiviral effect activity against orthohantavirus. Other studies have shown that fucoidan has stronger anti-pathogenic activity at higher molecular weights [15]. For example, the antiviral activity of fucoidan from *Fucus evanescens* against herpes simplex virus (HSV) was increased with increasing molecular weight [16]. Pathogen infections including bacteria and viruses cause a serious threat to human health and life. However, the size-dependent activities of fucoidan in inhibiting pathogen infections remain unclear due to complex and diverse structures of

* Corresponding author at: School of Food Science and Technology, Dalian Polytechnic University, No.1 Qinggongyuan, Ganjingzi district, Dalian 116034, PR China.
E-mail address: songs1008@163.com (S. Song).

https://doi.org/10.1016/j.ijbiomac.2022.12.307
Received 11 November 2022; Received in revised form 23 December 2022; Accepted 27 December 2022
Available online 29 December 2022

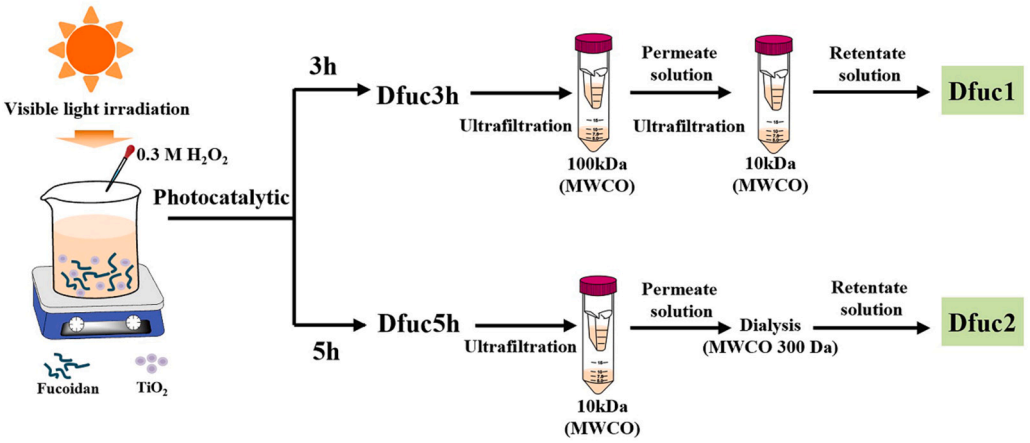

Fig. 1. Schematic diagram of the preparation of Dfuc1 and Dfuc2.

fucoidan. Therefore, more studies are urgently needed on the relationship between molecular weight and activity.

To date, various depolymerization methods for fucoidan include acid hydrolysis [8], oxidative degradation [17], enzymatic degradation [18], ultrasound and microwave degradation [1], etc. But these methods have some limitations in industrial production. Acid hydrolysis is a common method to degrade fucoidan, but it tends to damage the sulfate group of fucoidan and generate side products [17]. Enzymatic degradation is still relatively costly and unstable [19]. Ultrasonic or microwave degradation requires special equipments [20]. Noteworthily, photocatalytic degradation, as an eco-friendly technique, has attracted widespread attention. In our previous study, photocatalytic degradation was an effective, low-cost and easy-to-operate degradation method to depolymerize fucoidan and did not strip the sulfate groups [7]. However, the structural changes caused by photocatalytic reaction remain unclear. In this study, different molecular weight fucoidans were prepared by photocatalytic reaction followed by membrane ultrafiltration, and their structures were further elucidated by chemical composition analysis, FT-IR and NMR spectra. Furthermore, the antibacterial and antiviral activity of different molecular weight fucoidans were determined aiming to provide a better understanding of the relationship between structure and activity of fucoidan.

2. Materials and methods

2.1. Materials and chemical reagents

Fucoidan from *Laminaria japonica* was purchased by Rizhao Jiejing Ocean Biotechnology Development Co., Ltd. (Rizhao, China). Commercial TiO_2 NPs (P25) was obtained from Evonik Degussa Specialty Chemicals Co., Ltd. (Frankfurt, Germany) and the average particle size was about 20.9 ± 0.2 nm (see Method S1 and Fig. S1). All standard monosaccharides and standard dextran were provided by Sigma-Aldrich (St. Louis, MO, USA). Bacteria culture medium was acquired from Hope Bio. (Qingdao, China). All other chemicals and reagents were obtained from Aladdin (Shanghai, China).

2.2. Preparation of depolymerized fucoidans by photocatalytic degradation and membrane ultrafiltration

Photocatalytic degradation was conducted according to our previous method [7]. The reaction was performed in a reactor system (CEL-HXF300-T3, Beijing Au-light, Beijing, China) with a 300 W Xenon lamp as the simulation light source. Prior to irradiation, 1 g of the TiO_2 was dispersed in 200 mL 5 mg/mL fucoidan solution. Subsequently, H_2O_2 at a concentration of 0.3 M was added with magnetic stirring. The reaction temperature (room temperature, 23 ± 2 °C) was controlled using circulating water. After 3 h and 5 h of reaction, the suspension was separately centrifuged (10,000 rpm, 15 min) to remove the TiO_2 particles and the supernatant was collected as the photocatalytic degraded fucoidans, namely Dfuc3h and Dfuc5h, respectively. For further purification, Dfuc3h was fractionated by using membrane ultrafiltration with molecular weight cut-off (MWCO) of 100 kDa, and the 100 kDa permeate was further filtered through 10 kDa membrane. Then, the 10 kDa retentate was collated and named Dfuc1. Dfuc5h was fractionated with membrane ultrafiltration (10 kDa), and then the 10 kDa permeate was dialyzed (MWCO 300 Da) to obtain Dfuc2. Finally, Dfuc1 and Dfuc2 were freeze-dried for further chemical, antibacterial and antiviral analyses. The schematic diagram of Dfuc1 and Dfuc2 preparation was shown in Fig. 1.

2.3. Chemical composition analysis

The sulfate group content was analyzed by the $BaCl_2$-gelatin turbidity method [21]. The uronic acid content was estimated by the carbazole-sulfuric acid method [22]. The average molecular weight (Mw) was measured by an HPLC system (Waters, Milford, MA, USA) equipped with a TSK-GEL G5000PWXL column and a refractive index detector. Elution was performed with 100 mM ammonium acetate at a flow rate of 0.4 mL/min. Monosaccharide composition was determined by using 1-phenyl-3-methyl-5-pyrazolone (PMP) derivatization [23]. The derivatives were detected using HPLC (Thermo Fisher Scientific, Waltham, MA, USA) equipped with a photodiode array (PDA) detector and a Diamosil C18 column (250 mm × 4.6 mm, 5 μm). Elution was performed with 20 mM ammonium acetate- acetonitrile (86:14, v/v) at a flow rate of 1 mL/min.

2.4. FT-IR and NMR spectroscopy analysis

Samples were mixed with KBr and pressed into a disk. The FT-IR spectra were measured by a Perkin Elmer FT-IR Spectrometer (Perkin Elmer, Waltham, MA, USA) at room temperature. For NMR analysis, samples (45 mg) were dissolved in D_2O for repeated freeze-drying three times, and then redissolved in 500 μL of D_2O (99.9 %). The spectra of ^1H NMR, ^{13}C NMR, and HSQC were recorded on Bruker Avance III 400 NMR spectrometer (Bruker Biospin, Rheinstetten, Germany).

2.5. Antibacterial activity

2.5.1. Bacterial strain and culture conditions

Bacteria including *Staphylococcus aureus* ATCC6538, *Listeria monocytogenes* ATCC19115, *Escherichia coli* ATCC25922, *Shigella flexneri* CMCC51574, *Salmonella typhimurium* ATCC14028, and *Vibrio parahaemolyticus* CGMCC1.1614 were obtained from in our laboratory. All

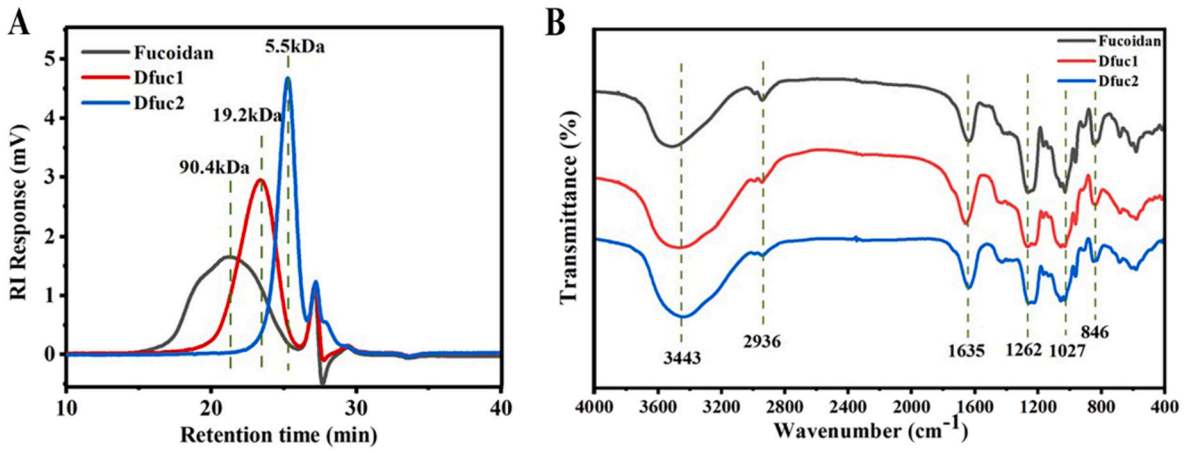

Fig. 2. Molecular weight distribution (A) and FT-IR spectra (B) of fucoidan, Dfuc1 and Dfuc2.

strains were cultured in LB broth medium at 37 °C for 12 h under shaking conditions.

2.5.2. Growth curve

The antimicrobial activity of fucoidan samples (fucoidan, Dfuc1 and Dfuc2) was measured by turbidimetry assay [24] with Bioscreen C Microbiology Reader (Labsystems, Helsinki, Finland). All strains were cultured to the mid-log phase and the suspensions were adjusted to approximately 1×10^6 CFU/mL in fresh LB medium. The fucoidan samples were added to the cultures to obtain a final concentration of 5 mg/mL. The cultures were incubated in the Bioscreen C automated growth curve analysis system at 37 °C with shaking, and the OD_{600nm} was measured every 2 h for 18 h. Bacterial cultures in free LB medium were set as control.

2.6. Anti-adherence activity

HT-29 cells were cultured in DMEM medium (Biological Industries, Kibbutz Beit-Haemek, Israel) containing 10 % fetal bovine serum and 1 % antibiotic solution, and were maintained with 5 % CO_2 atmosphere at 37 °C. The cell adhesion experiment was analyzed as previous methods [25]. Briefly, HT-29 cells (1×10^5 cells/well) were seeded in 24-well plates, and the plates were cultured in the incubator until a cell monolayer was obtained. The bacteria were collected by centrifuging (8000 rpm, 5 min), washed twice with PBS, and resuspended in the DMEM medium (without antibiotics) to approximately 2.0×10^8 CFU/mL. Then, 500 μL of the bacterial suspension and 500 μL of fucoidan samples solutions (final concentrations of 1, 2 and 5 mg/mL) were added into the 24-well plate. Cell cultures in fresh DMEM medium (without antibiotics) were set as control. After incubation for 2 h, the cells were washed three times with PBS, and lysed by 0.5 % TritonX-100 for 20 min. The amounts of adherent bacteria were measured on LB agar by the plate counting method.

2.7. Virus neutralization assay

The experiment was performed in a biological safety protection third-level laboratory of Naval Medical University as our previous description [26]. Briefly, HeLa cells (1×10^4 cells/well) were seeded in 96-well plates and cultured overnight. Then, 50 μL of fucoidan samples at different concentrations and 50 μL of the SARS-CoV-2 virus were added into the wells maintaining for 24 h. The virus infection was detected by indirect immunofluorescent assay, the images were obtained by Biotek Cytation 5 Cell Imaging Reader, and fluorescence intensity was calculated using image J.

Table 1
Chemical compositions of fucoidan, Dfuc1 and Dfuc2.

Sample	Sulfate group[1] (%)	Uronic acid content (%)	Main monosaccharides[2] (molar ratio)
			Fuc:Gal:Man
Fucoidan	28.7 ± 2.6[a]	16.2 ± 0.4	5.9:1.4:1.0
Dfuc1	24.7 ± 0.9[b]	15.0 ± 0.6	5.6:1.2:1.0
Dfuc2	23.3 ± 1.0[b]	15.5 ± 1.0	3.1:1.0:1.0

[1] Different superscript letters represent the statistically significant differences ($p < 0.05$).
[2] Molar ratio is expressed as relative to Man.

2.8. ACE2 competition ELISA assay

To evaluate whether fucoidan, Dfuc1 and Dfuc2 could block the interaction between human Angiotensin I Converting Enzyme 2 (hACE2) and Spike Receptor Binding Domain (RBD), the hACE2 competition ELISA was carried out by using the SARS-CoV-2 (WT) Inhibitor Screening Kit (Spike RBD) (ACROBiosystems, Beijing, China) according to the instructions. SARS-CoV-2 Inhibitor was set as positive control (ACROBiosystems, Beijing, China), HRP-conjugated SARS-CoV-2 RBD was set as control, and dilution buffer was set as blank. The absorbance at 450 nm was determined using a microplate reader (Tecan, Männedorf, Switzerland). The percent activity was calculated as follows:

$$\text{Percent activity } (\%) = \left(\text{Abs}_{\text{sample}} - \text{Abs}_{\text{blank}}\right) / \left(\text{Abs}_{\text{control}} - \text{Abs}_{\text{blank}}\right) \times 100$$

2.9. Statistical analysis

All data were expressed as mean ± standard error (SD). Student's *t*-test and one-way ANOVA were used for statistical analysis. Moreover, Duncan's test (data obey homogeneity of variance) or Dunnett's T3 test (data do not obey homogeneity of variance) was applied to multiple comparisons, and $p < 0.05$ was indicated statistically significant.

3. Results and discussion

3.1. Composition analysis

In the present study, fucoidan was depolymerized by photocatalytic reaction under visual light irradiation, and then the depolymerized products of fucoidan were further purified by using ultrafiltration to obtain Dfuc1 and Dfuc2. From the XPS analysis (Fig. S2), no obvious Ti element was observed in either Dfuc1 or Dfuc2. The average Mw of Dfuc1 and Dfuc2 were 19.2 kDa and 5.5 kDa, respectively (Fig. 2A).

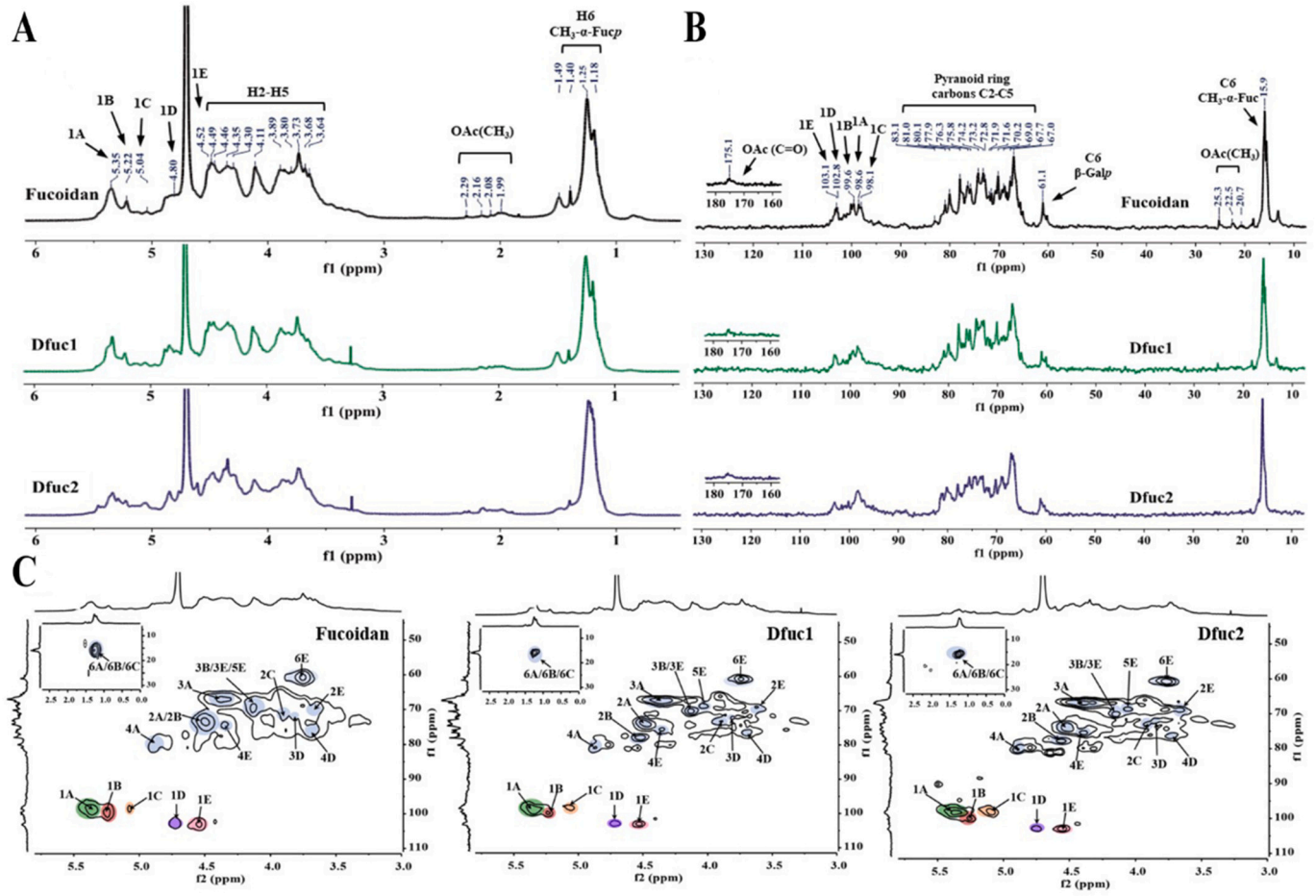

Fig. 3. ^{1}H NMR spectra (A), ^{13}C NMR spectra (B), and HSQC spectra(C) of fucoidan, Dfuc1 and Dfuc2.

Compared to the native fucoidan, the sulfate group content of Dfuc1 and Dfuc2 have slightly decreased, their uronic acids content were both around 15 % and have no significant variations among fucoidan (Table 1). The monosaccharide composition of fucoidan, Dfuc1 and Dfuc2 was similar, mainly composed of fucose, galactose and mannose, and a smaller percentage of xylose, arabinose, rhamnose and glucuronic acid (Table 1 and Fig. S3), indicating that the depolymerized reaction did not change the monosaccharide types. But the proportion of fucose, galactose and mannose obviously different, and the proportion of fucose reduced in Dfuc2, which may be due to partial loss of fucose residues after dialysis.

3.2. FT-IR

To identify the structural changes of fucoidan during degradation process, FT-IR spectra of fucoidan, Dfuc1 and Dfuc2 were compared as illustrated in Fig. 2B. Both native and low-molecular-weight fucoidan samples displayed similar spectral bands, and the function groups of fucoidan samples did not obviously change with decreasing molecular weight. The absorbance bands at approximately 3443 cm^{-1} and 2936 cm^{-1} were respectively attributed to the O—H and C—H stretching vibrations. The absorbance band at 1635 cm^{-1} was attributed to the C═O of uronic acids. The absorbance bands around 1262 cm^{-1} and 846 cm^{-1} were assigned to the stretching vibration S═O and C-O-S of sulfate group, respectively [27,28]. Therefore, these results suggest that there are no significant differences in function groups among fucoidan, Dfuc1 and Dfuc2.

3.3. NMR spectroscopy analysis

To further explore the information on structural changes, fucoidan, Dfuc1 and Dfuc2 were investigated by NMR spectroscopy. In the 1D NMR spectra (Fig. 3A and B), several intense signals in α-anomeric regions (δ_{H1} 5.0–5.5, δ_{C1} 94–100) and the strong signals in high-field region (δ_{H6} 1.2–1.4, δ_{C6} 15–17) were observed, which were characteristic signal of α-L-fucopyranose residues [29]. The carbon signals around δ_{C1} 103.07, δ_{C6} 67.02 (CH_2OR) and δ_{C6} 61.07 (CH_2OH) could be ascribed to β-D-galactopyranose residues [2]. The small carbon signals at δ_C 175.1 and δ_C 20.7–21.2 were assigned to carbonyl carbon (C=O) and *O*-acetyl groups, respectively [30]. In general, Dfuc1 and Dfuc2 demonstrated characteristic signals similar to those of fucoidan.

Further, the HSQC spectrum (Fig. 3C) combined with previously reported literatures [31–34], some assignments of ^{1}H and ^{13}C chemicals shifts are shown in Table 2. For fucoidan, there were some signals for the α-L-fucose moiety, the cross peaks at 5.36/98.9 ppm (residue A), 5.24/99.7 ppm (residue B) and 5.08/98.3 ppm (residue C) were identified to →3)-α-L-Fuc*p*(2,4*S*)-(1→, →3)-α-L-Fuc*p*(2*S*)-(1→ and →3)-α-L-Fuc*p*-(1→, respectively. In addition, the signal at 4.72/102.8 ppm (residue D) was attributed to →4)-β-D-Manp(1→ and the signal at 4.54/103.0 ppm (residue E) was assigned to →6)-β-D-Galp(1→. For Dfuc1 and Dfuc2, there were no significant spectral changes in α-anomeric regions, which suggests fucoidan, Dfuc1 and Dfuc2 possess common monosaccharide residues. Besides, there were more signal peaks in C2-C5 regions, possibly due to higher water solubility of degraded products with the reduction of molecular weight [35]. As indicated by the above results, the backbone of fucoidan was mainly constructed of 1,3-linked-α-L-fucose residues sulfated at C2 and/or C4, 1,4-linked β-D-mannose

Table 2
Assignments of ^{1}H and ^{13}C NMR signals of fucoidan, Dfuc1 and Dfuc2.

Sample	Residue	Chemical shift (ppm)					
		H1/ C1	H2/ C2	H3/ C3	H4/ C4	H5/ C5	H6/ C6
Fucoidan	A:→3)-α-L-Fucp (2,4*S*)-(1→	5.36/ 98.9	4.50/ 73.6	4.33/ 66.8	4.88/ 80.5	–	1.23/ 15.9
	B:→3)-α-L-Fucp(2*S*)-(1→	5.24/ 99.7	4.57/ 74.2	4.14/ 70.0	–	–	1.23/ 15.9
	C:→3)-α-L-Fucp-(1→	5.08/ 98.3	3.91/ 72.8	–	–	–	1.23/ 15.9
	D:→4)-β-D-Manp(1→	4.72/ 102.8	–	3.83/ 72.0	3.70/ 76.4	–	–
	E:→6)-β-D-Galp(1→	4.54/ 103.0	3.68/ 70.9	4.11/ 68.9	4.34/ 74.5	4.08/ 67.9	3.76/ 60.7
Dfuc1	A:→3)-α-L-Fucp (2,4*S*)-(1→	5.34/ 99.0	4.54/ 80.9	4.36/ 67.1	4.86/ 80.8	–	1.24/ 15.9
	B:→3)-α-L-Fucp(2*S*)-(1→	5.24/ 99.6	4.52/ 77.9	4.15/ 70.2	–	–	1.24/ 15.9
	C:→3)-α-L-Fucp-(1→	5.06/ 98.3	3.93/ 72.7	–	–	–	1.24/ 15.9
	D:→4)-β-D-Manp(1→	4.72/ 102.8	–	3.83/ 72.0	3.70/ 76.4	–	–
	E:→6)-β-D-Galp(1→	4.53/ 103.0	3.68/ 70.9	4.11/ 68.9	4.39/ 75.4	4.06/ 68.7	3.74/ 60.8
Dfuc2	A:→3)-α-L-Fucp (2,4*S*)-(1→	5.37/ 98.3	4.51/ 73.8	4.33/ 66.8	4.89/ 80.4	–	1.23/ 15.9
	B:→3)-α-L-Fucp(2*S*)-(1→	5.24/ 99.7	4.56/ 77.8	4.15/ 70.1	–	–	1.23/ 15.9
	C:→3)-α-L-Fucp-(1→	5.09/ 98.1	3.91/ 71.9	–	–	–	1.23/ 15.9
	D:→4)-β-D-Manp(1→	4.75/ 102.8	–	3.86/ 72.1	3.74/ 76.4	–	–
	E:→6)-β-D-Galpn1→	4.56/ 102.9	3.68/ 70.9	4.11/ 68.9	4.39/ 75.4	4.08/ 67.9	3.76/ 60.7

residues and 1,6-linked β-D-galactose residues. In addition, the structure of Dfuc1 and Dfuc2 maintained the same backbone as that of the native fucoidan.

Based on the results from chemical composition analysis, FT-IR and NMR spectra, it was concluded that photocatalytic degradation could effectively depolymerize fucoidan, and the structure block and sulfate groups were not destroyed with decreasing molecular weight. In conclusion, except for varies in the molecular weight, it could be inferred that the fucoidan, Dfuc1 and Dfuc2 shared similar structural features.

3.4. Influence of molecular weight on inhibitory effect of fucoidan on pathogenic bacteria

The antibacterial activity of fucoidan, Dfuc1 and Dfuc2 were evaluated against some common food pathogens, including Gram-negative (*E. coli*, *S. flexneri*, *S. typhimurium* and *V. parahaemolyticus*) and Gram-positive (*L. monocytogenes* and *S. aureus*) bacteria. As presented in Fig. 4, fucoidan, Dfuc1 and Dfuc2 showed different inhibitory capabilities toward the tested bacterial strains, and antibacterial activity of fucoidan was superior to that of its depolymerized products. After 18 h of incubation, fucoidan (5 mg/mL) could inhibit the growth of *S. aureus*, *S. typhimurium* and *E. coli* with the inhibition rates of 25.9 ± 1.0 %, 24.1 ± 2.8 %, 13.2 ± 2.7 %, respectively, while Dfuc2 was only slightly inhibitory activity against *S. typhimurium*. It has been reported that the <10 kDa fucoidan fraction exerted a slightly weaker antibacterial effect on *B. subtilis* and *P. fluorescens* than other high-molecular-weight fractionation at low concentrations [36]. Moreover, a non-depolymerized sulfated polysaccharide from smooth hound viscera exhibited higher and wide spectrum of antimicrobial activities at 20 mg/mL than that of low-molecular-weight fragment [37]. These results implied that molecular weight is one of the key factors to determine the antimicrobial activities, and stronger antibacterial activity of fucoidan is possibly due to its higher molecular weight. However, in the study of Liu et al. [13], the fucoidan from *Laminaria japonica* has no influence on the growth of *E. coli* and *S. aureus*, while depolymerized fucoidan (<6 kDa) exhibited

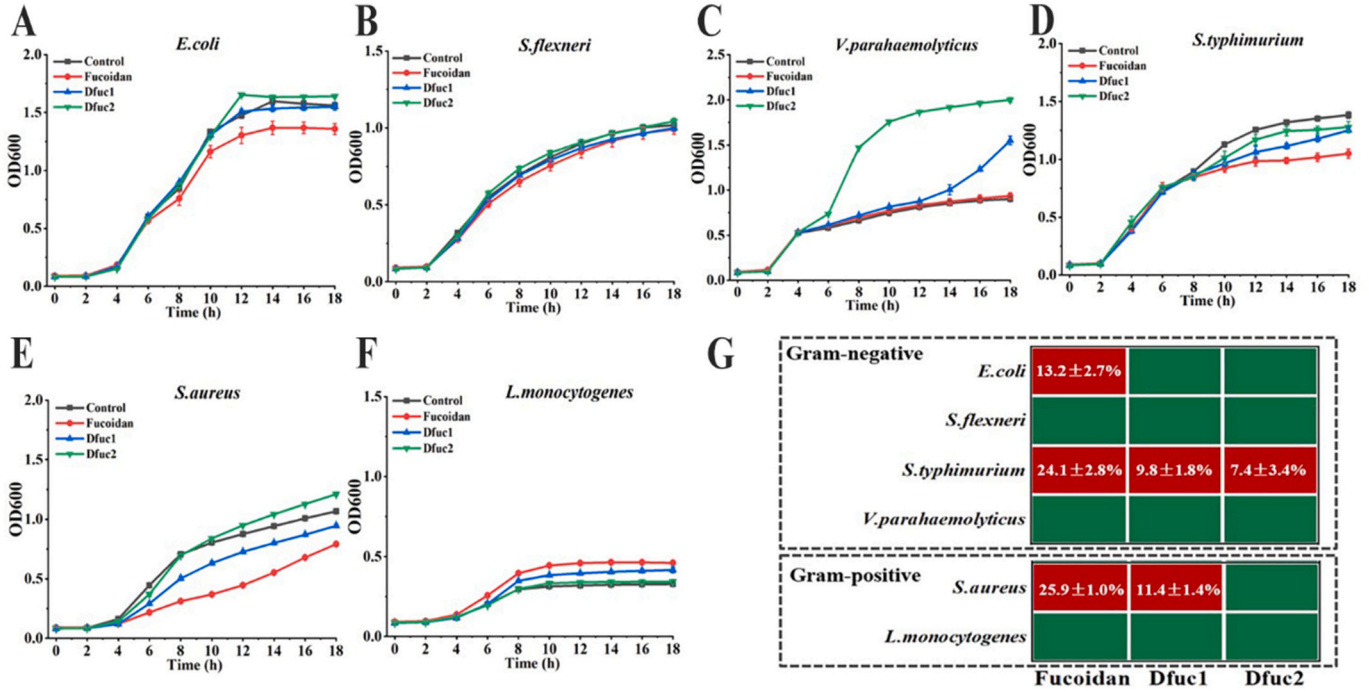

Fig. 4. Effect of fucoidan, Dfuc1 and Dfuc2 on the growth of *E. coli* (A), *S. flexneri* (B), *V. parahaemolyticus* (C), *S. typhimurium* (D), *S. aureus* (E), and *L. monocytogenes* (F), and the effects of fucoidan, Dfuc1 and Dfuc2 were summarized in (G). The red and green squares represent significant inhibitory effect and no effect, respectively. (For interpretation of the references to colour in this figure legend, the reader is referred to the web version of this article.)

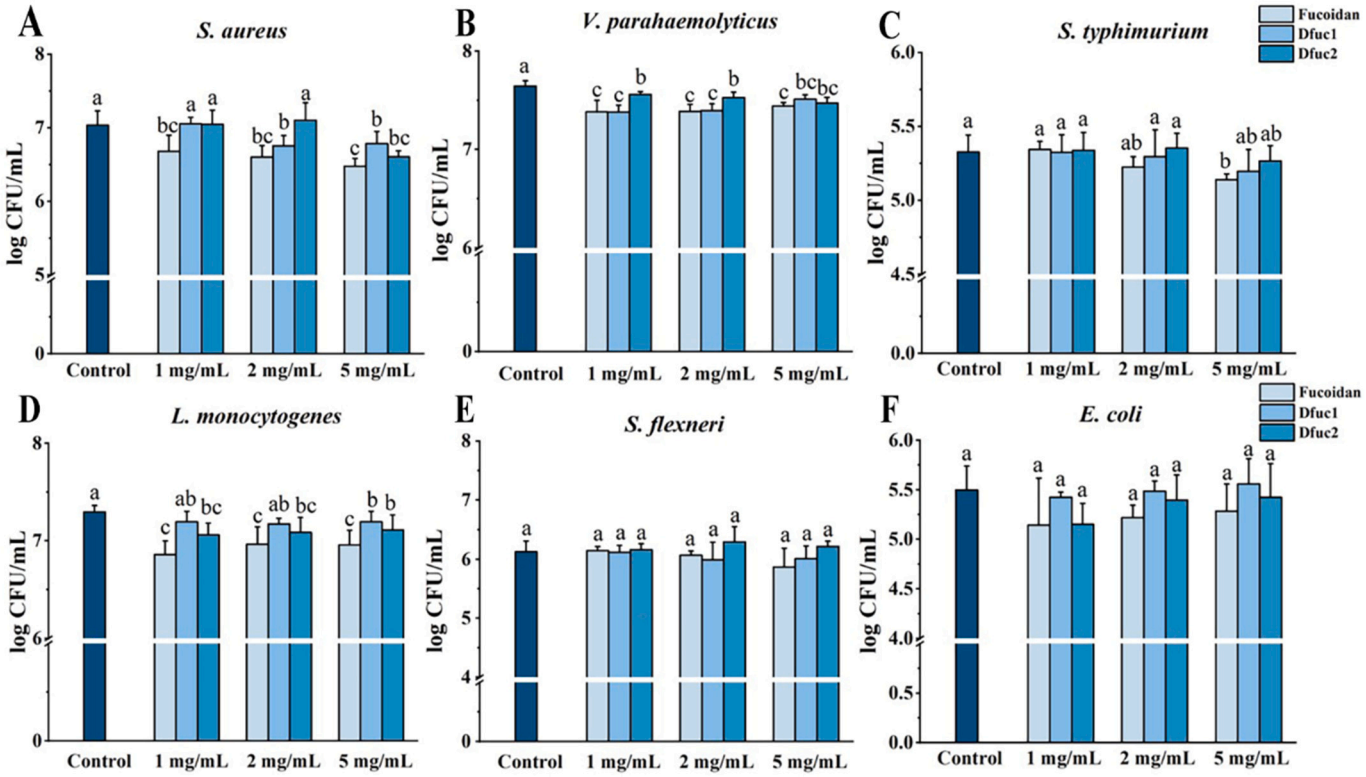

Fig. 5. Effect of fucoidan, Dfuc1 and Dfuc2 on the adherence of foodborne pathogens to HT-29 cells cultures. (A) *S. aureus,* (B) *V. parahaemolyticus,* (C) *S. typhimurium,* (D) *L. monocytogenes,* (E) *S. flexneri,* (F). *E. coli.* Different letters represent the statistically significant differences ($p < 0.05$).

effectively inhibitory effect. It was contrary to the results of our findings that the antibacterial activity of fucoidan from *Laminaria japonica* was decreased along with the reduction of molecular weight. This discrepancy may be due to the differences of the studied fucoidans in chemical structures which could be varied with polysaccharide isolation methods and algae growth [3,38].

3.5. Influence of molecular weight on inhibition of fucoidan against the adhesion of pathogenic bacteria

Bacterial adhesion to the tissues of the host is the prerequisite for the initiation of the majority of infectious diseases [39]. The human colonic epithelial cell line HT-29 was used to evaluate the adhesion ability of six food pathogens. All strains had the capacity to adhere to HT-29 cells, and the level of adhesion varied among the bacteria. In addition, fucoidan, Dfuc1 and Dfuc2 showed no cytotoxicity at the concentrations studied (Fig. S4). Compared to the control, fucoidan, Dfuc1 and Dfuc2 significantly inhibited the adhesion of *S. aureus*, *L. monocytogenes*, *V. parahaemolyticus* and *S. typhimurium*, while no influence on the adhesion of *E. coli* and *S. flexneri*. These results suggest that fucoidan and its degradation products could selectively reduce some pathogen adhesion (Fig. 5). Previous studies have reported that some polysaccharides and oligosaccharides could prevent the cellular adhesion by pathogens to human colonic epithelial cells [40–42]. In particular, heparin and

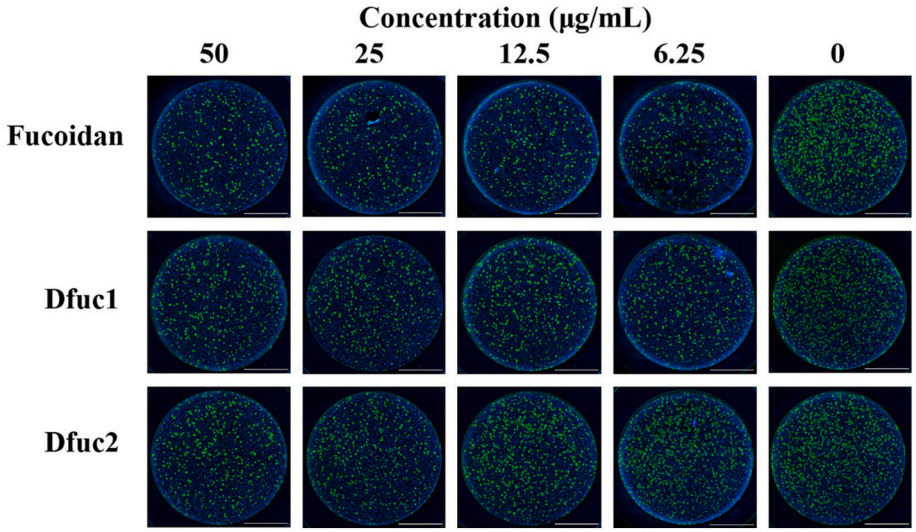

Fig. 6. Inhibitory activity of fucoidan, Dfuc1 and Dfuc2 against SARS-CoV-2.

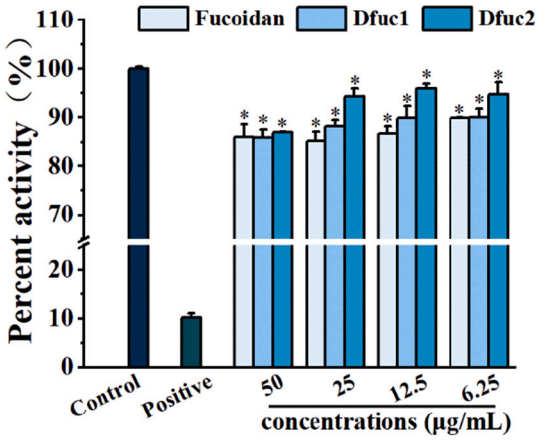

Fig. 7. Effect of fucoidan, Dfuc1 and Dfuc2 on binding between SARS-CoV-2 S protein RBD and ACE2 by ELISA assay. *$p < 0.05$, as compared with the control group.

heparin-like sulfated polysaccharides have been confirmed to modulate bacteria-epithelial binding due to their negatively charged structure similar to heparan sulfate at cell surface [43,44]. Similarly, highly sulfated fucoidan or its degradation products could also bind to bacteria in competition with heparin-like moieties and thus block pathogens attachment to the host cell.

Notably, fucoidan, Dfuc1 and Dfuc2 showed different anti-adhesion activities, and fucoidan had stronger inhibition ability than Dfuc1 and Dfuc2, especially for *S. aureus* and L. *monocytogenes* (Fig. 5). It implied that the anti-pathogenic activity of fucoidan is closely associated with their molecular size. Previous studies revealed that pectin-like acidic polysaccharide from *Panax ginseng* could effectively inhibit the adherence of pathogens to KB cells, while the anti-adhesive activity is lost after enzymatic hydrolysis [45]. However, another study showed that compared to the pectin, pectic oligosaccharides had higher anti-adhesion activity against *E. coli* [46]. Although the structure-bioactive relationships of anti-pathogenic polysaccharides are complicated, it is confirmed that molecular weight plays an important role in the anti-adhesion.

3.6. Influence of molecular weight on inhibitory effect of fucoidan against SARS-CoV-2

Viral infection is also considered as one of the great threats to human health. To confirm the inhibitory effect against SARS-CoV-2 virus, the virus neutralization assay was conducted (Fig. 6). Fucoidan, Dfuc1 and Dfuc2 effectively inhibited SARS-CoV-2 infection on HeLa cells at concentrations of 6.25–50 μg/mL, and fucoidan demonstrated the strongest inhibitory activity, followed by Dfuc1 and then Dfuc2. To date, some sulfated polysaccharides from brown seaweeds, including fucoidan, have shown promising anti-SARS-CoV-2 activity, due to their unique structure and high sulfation degree [47,48]. However, the present study demonstrated that the inhibitory effect decreased along with reduction of the molecule weight when the sulfation degree has no significant difference, implying that the molecular weight is a crucial factor in influencing the antiviral activity of polysaccharides. This finding is consistent with the previous report that high-molecular-weight sulfated galactofucans from *Saccharina japonica* showed stronger antiviral activity than that of its low-molecular-weight fragment [49].

It has been reported that fucoidan could competitively inhibit the binding between heparan sulfate and SARS-CoV-2 S protein so to inhibit the infection of SARS-CoV-2 [50,51]. Thus, in order to further explain the different capabilities against SARS-CoV-2 among fucoidan, Dfuc1 and Dfuc2, they were screened by interfering binding between SARS-CoV-2 S protein RBD and ACE2. All of them could impede the binding of S protein and ACE2, and the binding activity to S protein is positively correlated to fucoidan molecular weight (Fig. 7). This is consistent with the previous study that sulfated galactan from *Botryocladia occidentalis* demonstrated better binding affinity to the SARS-CoV-2 S protein compared to its depolymerization products [52]. Therefore, these results reveal that fucoidan with higher molecular weight could more effectively block with S protein binding to host receptor ACE2 so possesses stronger inhibitory activity.

Many studies showed that low-molecular-weight fucoidan had better biological activity, such as anti-cancer [6], while fucoidan had higher inhibitory effect against these pathogens compared to Dfuc1 and Dfuc2 in the present study. The different effect of molecular weight of fucoidan on the bioactivities could be attributed to the different action mechanisms. Low-molecular-weight fucoidan is easier to enter cells, so it has stronger anti-cancer activity via induction of cell cycle arrest, apoptosis and immune system activation [53,54]. However, in term of anti-pathogenic activity, fucoidan with longer chain has more chance to cover the surface of these pathogens to prevent the absorption of nutrients then leading to these pathogens growth inhibition [55,56]. Therefore, it is necessary to explore the relationship between structure and activity of fucoidan in various functions.

4. Conclusion

This study showed that photocatalytic degradation did not destroy the structure block and sulfate groups of fucoidan obviously. Compared to Dfuc1 and Dfuc2, fucoidan had better anti-bacterial and anti-adhesion activities, especially for *S. aureus*. In addition, fucoidan demonstrated the highest inhibitory effect SARS-CoV-2 infection on HeLa cells, followed by Dfuc1, and then Dfuc2. Therefore, natural fucoidan with higher molecular weight could more effectively inhibit some pathogenic bacteria and SARS-CoV-2, and providing a better understanding of the relationship between structure and activity of fucoidan against pathogenic microbiota.

CRediT authorship contribution statement

Xiaona Sun: Data curation, Writing – original draft. **Chunqing Ai:** Investigation, Formal analysis. **Chengrong Wen:** Conceptualization, Supervision. **Haoran Peng:** Methodology. **Jingfeng Yang:** Investigation, Resources. **Yuna Cui:** Supervision, Resources. **Shuang Song:** Supervision, Writing – review & editing, Project administration, Funding acquisition.

Declaration of competing interest

The authors declare that we have no known competing financial interests or personal relationships that could have appeared to influence the work reported in this paper.

Acknowledgements

This work was supported by the National Key Research and Development Program of China (No. 2019YFD0902005) and the Graduate Innovation Fund of Dalian Polytechnic University.

Appendix A. Supplementary data

Supplementary data to this article can be found online at https://doi.org/10.1016/j.ijbiomac.2022.12.307.

References

[1] N. Flórez-Fernández, M.D. Torres, M.J. González-Muñoz, H. Domínguez, Potential of intensification techniques for the extraction and depolymerization of fucoidan, Algal Res. 30 (2018) 128–148, https://doi.org/10.1016/j.algal.2018.01.002.

[2] O.S. Vishchuk, S.P. Ermakova, T.N. Zvyagintseva, Sulfated polysaccharides from brown seaweeds Saccharina japonica and Undaria pinnatifida: isolation, structural characteristics, and antitumor activity, Carbohydr. Res. 346 (17) (2011) 2769–2776, https://doi.org/10.1016/j.carres.2011.09.034.
[3] M. Alboofetileh, M. Rezaei, M. Tabarsa, M. Rittà, M. Donalisio, F. Mariatti, S. You, D. Lembo, G. Cravotto, Effect of different non-conventional extraction methods on the antibacterial and antiviral activity of fucoidans extracted from Nizamuddinia zanardinii, Int. J. Biol. Macromol. 124 (2019) 131–137, https://doi.org/10.1016/j.ijbiomac.2018.11.201.
[4] Y. Wang, M. Xing, Q. Cao, A. Ji, H. Liang, S. Song, Biological activities of fucoidan and the factors mediating its therapeutic effects: a review of recent studies, Mar. Drugs 17 (3) (2019) 183, https://doi.org/10.3390/md17030183.
[5] T. Zhang, S. Wu, C. Ai, C. Wen, Z. Liu, L. Wang, L. Jiang, P. Shen, G. Zhang, S. Song, Galactofucan from Laminaria japonica is not degraded by the human digestive system but inhibits pancreatic lipase and modifies the intestinal microbiota, Int. J. Biol. Macromol. 166 (2021) 611–620, https://doi.org/10.1016/j.ijbiomac.2020.10.219.
[6] H.L. Tsai, C.J. Tai, C.W. Huang, F.R. Chang, J.Y. Wang, Efficacy of low-molecular-weight fucoidan as a supplemental therapy in metastatic volorectal cancer patients: a double-blind randomized controlled trial, Mar. Drugs 15 (4) (2017) 122, https://doi.org/10.3390/md15040122.
[7] Y. Qi, L. Wang, Y. You, X. Sun, C. Wen, Y. Fu, S. Song, Preparation of low-molecular-weight fucoidan with anticoagulant activity by photocatalytic degradation method, Foods 11 (6) (2022) 822, https://doi.org/10.3390/foods11060822.
[8] T.C. Wu, Y.H. Hong, Y.H. Tsai, S.L. Hsieh, R.H. Huang, C.H. Kuo, C.Y. Huang, Degradation of Sargassum crassifolium fucoidan by ascorbic acid and hydrogen peroxide, and compositional, structural, and in vitro anti-lung cancer analyses of the degradation products, Mar. Drugs 18 (6) (2020) 334, https://doi.org/10.3390/md18060334.
[9] W.C. Hsiao, Y.H. Hong, Y.H. Tsai, Y.C. Lee, A.K. Patel, H.R. Guo, C.H. Kuo, C. Y. Huang, Extraction, Biochemical characterization, and health effects of native and degraded fucoidans from Sargassum crispifolium, Polymers (Basel) 14 (9) (2022) 1812, https://doi.org/10.3390/polym14091812.
[10] O.N. Pozharitskaya, E.D. Obluchinskaya, A.N. Shikov, Mechanisms of bioactivities of fucoidan from the brown seaweed Fucus vesiculosus L. of the barents sea, Mar. Drugs 18 (5) (2020) 275, https://doi.org/10.3390/md18050275.
[11] T.N. Zvyagintseva, R.V. Usoltseva, N. Shevchenko, V.V. Surits, T.I. Imbs, O. S. Malyarenko, N.N. Besednova, L.A. Ivanushko, S.P. Ermakova, Structural diversity of fucoidans and their radioprotective effect, Carbohydr. Polym. 273 (2021), 118551, https://doi.org/10.1016/j.carbpol.2021.118551.
[12] Q. Guo, X. Huang, J. Kang, H.H. Ding, Y. Liu, N. Wang, S.W. Cui, Immunomodulatory and antivirus activities of bioactive polysaccharides and structure-function relationship, Bioact. Carbohydr. Diet. Fibre 27 (2022), 100301, https://doi.org/10.1016/j.bcdf.2021.100301.
[13] M. Liu, Y. Liu, M.J. Cao, G.M. Liu, Q. Chen, L. Sun, H. Chen, Antibacterial activity and mechanisms of depolymerized fucoidans isolated from Laminaria japonica, Carbohydr. Polym. 172 (2017) 294–305, https://doi.org/10.1016/j.carbpol.2017.05.060.
[14] N.V. Krylova, A.S. Silchenko, A.B. Pott, S.P. Ermakova, O.V. Iunikhina, A.B. Rasin, G.G. Kompanets, G.N. Likhatskaya, M.Y. Shchelkanov, In vitro anti-orthohantavirus activity of the high-and low-molecular-weight fractions of fucoidan from the brown alga Fucus evanescens, Mar. Drugs 19 (10) (2021) 577, https://doi.org/10.3390/md19100577.
[15] T. Ghosh, K. Chattopadhyay, M. Marschall, P. Karmakar, P. Mandal, B. Ray, Focus on antivirally active sulfated polysaccharides: from structure-activity analysis to clinical evaluation, Glycobiology 19 (1) (2008) 2–15, https://doi.org/10.1093/glycob/cwn092.
[16] N.V. Krylova, S.P. Ermakova, V.F. Lavrov, I.A. Leneva, G.G. Kompanets, O. V. Iunikhina, M.N. Nosik, L.K. Ebralidze, I.N. Falynskova, A.S. Silchenko, T. S. Zaporozhets, The comparative analysis of antiviral activity of native and modified fucoidans from brown algae Fucus evanescens in vitro and in vivo, Mar. Drugs 18 (4) (2020) 224, https://doi.org/10.3390/md18040224.
[17] B.W. Jo, S.-K. Choi, Degradation of fucoidans from Sargassum fulvellum and their biological activities, Carbohydr. Polym. 111 (2014) 822–829, https://doi.org/10.1016/j.carbpol.2014.05.049.
[18] W. Yao, M. Liu, X. Chen, L. You, Y. Ma, K. Hileuskaya, Effects of UV/H2O2 degradation and step gradient ethanol precipitation on Sargassum fusiforme polysaccharides: physicochemical characterization and protective effects against intestinal epithelial injury, Food Res. Int. 155 (2022), 111093, https://doi.org/10.1016/j.foodres.2022.111093.
[19] X. Li, B. Peng, P. Chi-Keung Cheung, J. Wang, X. Zheng, L. You, Depolymerized non-digestible sulfated algal polysaccharides produced by hydrothermal treatment with enhanced bacterial fermentation characteristics, Food Hydrocoll. 130 (2022), 107687, https://doi.org/10.1016/j.foodhyd.2022.107687.
[20] W. Tian, Y. You, X. Sun, L. Wang, L. Wang, S. Wang, C. Ai, S. Song, H2O2-TiO2 photocatalytic degradation of chondroitin sulfate and in vivo absorption and excertion of its product, Carbohydr. Polym. 301 (2023), 120295, https://doi.org/10.1016/j.carbpol.2022.120295.
[21] S. Song, B. Zhang, S. Wu, L. Huang, C. Ai, J. Pan, Y.C. Su, Z. Wang, C. Wen, Structural characterization and osteogenic bioactivity of a sulfated polysaccharide from pacific abalone (Haliotis discus hannai Ino), Carbohydr. Polym. 182 (2018) 207–214, https://doi.org/10.1016/j.carbpol.2017.11.022.
[22] J. Li, K. Kisara, S. Danielsson, M.E. Lindström, G. Gellerstedt, An improved methodology for the quantification of uronic acid units in xylans and other polysaccharides, Carbohydr. Res. 342 (11) (2007) 1442–1449, https://doi.org/10.1016/j.carres.2007.03.031.
[23] S. Song, S. Wu, C. Ai, X. Xu, Z. Zhu, C. Cao, J. Yang, C. Wen, Compositional analysis of sulfated polysaccharides from sea cucumber (Stichopus japonicus) released by autolysis reaction, Int. J. Biol. Macromol. 114 (2018) 420–425, https://doi.org/10.1016/j.ijbiomac.2018.03.137.
[24] J. Bi, C. Tian, J. Jiang, G.L. Zhang, H. Hao, H.M. Hou, Antibacterial activity and potential application in food packaging of peptides derived from Turbot Viscera Hydrolysate, J. Agric. Food Chem. 68 (37) (2020) 9968–9977, https://doi.org/10.1021/acs.jafc.0c03146.
[25] Y. Song, M. Sun, L. Feng, X. Liang, X. Song, G. Mu, Y. Tuo, S. Jiang, F. Qian, Antibiofilm activity of Lactobacillus plantarum 12 exopolysaccharides against Shigella flexneri, Appl. Environ. Microbiol. 86 (15) (2020), e00694-20, https://doi.org/10.1128/aem.00694-20.
[26] S. Song, H. Peng, Q. Wang, Z. Liu, X. Dong, C. Wen, C. Ai, Y. Zhang, Z. Wang, B. Zhu, Inhibitory activities of marine sulfated polysaccharides against SARS-CoV-2, Food Funct. 11 (9) (2020) 7415–7420, https://doi.org/10.1039/d0fo02017f.
[27] B. Matsuhiro, Vibrational spectroscopy of seaweed galactans, Hydrobiologia 326 (1) (1996) 481–489, https://doi.org/10.1007/BF00047849.
[28] E. Gómez-Ordóñez, P. Rupérez, FTIR-ATR spectroscopy as a tool for polysaccharide identification in edible brown and red seaweeds, Food Hydrocoll. 25 (6) (2011) 1514–1520, https://doi.org/10.1016/j.foodhyd.2011.02.009.
[29] Y. Yang, T. Hu, J. Li, M. Xin, X. Zhao, Structural characterization and effect on leukopenia of fucoidan from Durvillaea antarctica, Carbohydr. Polym. 256 (2021), 117529, https://doi.org/10.1016/j.carbpol.2020.117529.
[30] S. Song, L. Wang, L. Wang, Q. Yu, C. Ai, Y. Fu, C. Yan, C. Wen, Z. Zhu, Structural characterization and anticoagulant activity of two polysaccharides from Patinopecten yessoensis viscera, Int. J. Biol. Macromol. 136 (2019) 579–585, https://doi.org/10.1016/j.ijbiomac.2019.06.116.
[31] M.I. Bilan, A.A. Grachev, N.E. Ustuzhanina, A.S. Shashkov, N.E. Nifantiev, A. I. Usov, Structure of a fucoidan from the brown seaweed Fucus evanescens C.Ag, Carbohydr. Res. 337 (8) (2002) 719–730, https://doi.org/10.1016/s0008-6215(02)00053-8.
[32] Y. Sun, Z. Liu, S. Song, B. Zhu, L. Zhao, J. Jiang, N. Liu, J. Wang, X. Chen, Anti-inflammatory activity and structural identification of a sulfated polysaccharide CLGP4 from Caulerpa lentillifera, Int. J. Biol. Macromol. 146 (2020) 931–938, https://doi.org/10.1016/j.ijbiomac.2019.09.216.
[33] J. Wang, Q. Zhang, Z. Zhang, H. Zhang, X. Niu, Structural studies on a novel fucogalactan sulfate extracted from the brown seaweed Laminaria japonica, Int. J. Biol. Macromol. 47 (2) (2010) 126–131, https://doi.org/10.1016/j.ijbiomac.2010.05.010.
[34] X. Wei, L. Cai, H. Liu, H. Tu, X. Xu, F. Zhou, L. Zhang, Chain conformation and biological activities of hyperbranched fucoidan derived from brown algae and its desulfated derivative, Carbohydr. Polym. 208 (2019) 86–96, https://doi.org/10.1016/j.carbpol.2018.12.060.
[35] X. Shen, Z. Liu, J. Li, D. Wu, M. Zhu, L. Yan, G. Mao, X. Ye, R.J. Linhardt, S. Chen, Development of low molecular weight heparin by H2O2/ascorbic acid with ultrasonic power and its anti-metastasis property, Int. J. Biol. Macromol. 133 (2019) 101–109, https://doi.org/10.1016/j.ijbiomac.2019.04.019.
[36] E.M. Cabral, J.R.M. Mondala, M. Oliveira, S. Fitzpatrick, D.K. Rai, S. P. Sivagnanam, M. Garcia-Vaquero, D. O'Shea, M. Devereux, B.K. Tiwari, J. Curtin, Influence of molecular weight fractionation on the antimicrobial and anticancer properties of a fucoidan rich-extract from the macroalgae Fucus vesiculosus, Int. J. Biol. Macromol. 186 (2021) 994–1002, https://doi.org/10.1016/j.ijbiomac.2021.06.182.
[37] O. Abdelhedi, R. Nasri, N. Souissi, M. Nasri, M. Jridi, Sulfated polysaccharides from common smooth hound: extraction and assessment of anti-ACE, antioxidant and antibacterial activities, Carbohydr. Polym. 152 (2016) 605–614, https://doi.org/10.1016/j.carbpol.2016.07.048.
[38] W. Mak, N. Hamid, T. Liu, J. Lu, W.L. White, Fucoidan from New Zealand Undaria pinnatifida: monthly variations and determination of antioxidant activities, Carbohydr. Polym. 95 (1) (2013) 606–614, https://doi.org/10.1016/j.carbpol.2013.02.047.
[39] N. Sharon, Carbohydrates as future anti-adhesion drugs for infectious diseases, Biochim. Biophys. Acta 1760 (4) (2006) 527–537, https://doi.org/10.1016/j.bbagen.2005.12.008.
[40] A.T. Hotchkiss Jr., A. Nunez, G.D. Strahan, H.K. Chau, A.K. White, J.P. Marais, K. Hom, M.S. Vakkalanka, R. Di, K.L. Yam, C. Khoo, Cranberry xyloglucan structure and inhibition of Escherichia coli adhesion to epithelial cells, J. Agric. Food Chem. 63 (23) (2015) 5622–5633, https://doi.org/10.1021/acs.jafc.5b00730.
[41] F.H. Al-Ghazzewi, R.F. Tester, Inhibition of the adhesion of Escherichia coli to human epithelial cells by carbohydrates, Bioact. Carbohydr. Diet. Fibre 4 (1) (2014) 1–5, https://doi.org/10.1016/j.bcdf.2014.05.001.
[42] M.V. Selma, M. Larrosa, D. Beltran, R. Lucas, J.C. Morales, F. Tomas-Barberan, J. C. Espin, Resveratrol and some glucosyl, glucosylacyl, and glucuronide derivatives reduce Escherichia coli O157:H7, Salmonella typhimurium, and Listeria monocytogenes Scott A adhesion to colonic epithelial cell lines, J. Agric. Food Chem. 60 (30) (2012) 7367–7374, https://doi.org/10.1021/jf203967u.
[43] L. Gu, H. Wang, Y.L. Guo, K. Zen, Heparin blocks the adhesion of E. coli O157:H7 to human colonic epithelial cells, Biochem. Biophys. Res. Commun. 369 (4) (2008) 1061–1064, https://doi.org/10.1016/j.bbrc.2008.02.160.
[44] P. Appelgren, U. Ransjo, L. Bindslev, F. Espersen, O. Larm, Surface heparinization of central venous catheters reduces microbial colonization in vitro and in vivo: results from a prospective, randomized trial, Crit. Care Med. 24 (9) (1996) 1482–1489, https://doi.org/10.1097/00003246-199609000-00009.

[45] J.H. Lee, J.S. Shim, M.S. Chung, S.T. Lim, K.H. Kim, Inhibition of pathogen adhesion to host cells by polysaccharides from Panax ginseng, Biosci. Biotechnol. Biochem. 73 (1) (2009) 209–212, https://doi.org/10.1271/bbb.80555.
[46] R. Di, M.S. Vakkalanka, C. Onumpai, H.K. Chau, A. White, R.A. Rastall, K. Yam, A. T. Hotchkiss Jr., Pectic oligosaccharide structure-function relationships: prebiotics, inhibitors of Escherichia coli O157:H7 adhesion and reduction of Shiga toxin cytotoxicity in HT29 cells, Food Chem. 227 (2017) 245–254, https://doi.org/10.1016/j.foodchem.2017.01.100.
[47] Y. You, H. Song, L. Wang, H. Peng, Y. Sun, C. Ai, C. Wen, B. Zhu, S. Song, Structural characterization and SARS-CoV-2 inhibitory activity of a sulfated polysaccharide from Caulerpa lentillifera, Carbohydr. Polym. 280 (2022), 119006, https://doi.org/10.1016/j.carbpol.2021.119006.
[48] B. Pradhan, R. Nayak, S. Patra, P.P. Bhuyan, P.K. Behera, A.K. Mandal, C. Behera, J.-S. Ki, S.P. Adhikary, D. MubarakAli, M. Jena, A state-of-the-art review on fucoidan as an antiviral agent to combat viral infections, Carbohydr. Polym. 291 (2022), 119551, https://doi.org/10.1016/j.carbpol.2022.119551.
[49] W. Jin, W. Zhang, D. Mitra, M.G. McCandless, P. Sharma, R. Tandon, F. Zhang, R. J. Linhardt, The structure-activity relationship of the interactions of SARS-CoV-2 spike glycoproteins with glucuronomannan and sulfated galactofucan from Saccharina japonica, Int. J. Biol. Macromol. 163 (2020) 1649–1658, https://doi.org/10.1016/j.ijbiomac.2020.09.184.
[50] T.M. Clausen, D.R. Sandoval, C.B. Spliid, J. Pihl, H.R. Perrett, C.D. Painter, A. Narayanan, S.A. Majowicz, E.M. Kwong, R.N. McVicar, B.E. Thacker, C.A. Glass, Z. Yang, J.L. Torres, G.J. Golden, P.L. Bartels, R.N. Porell, A.F. Garretson, L. Laubach, J. Feldman, X. Yin, Y. Pu, B.M. Hauser, T.M. Caradonna, B.P. Kellman, C. Martino, P. Gordts, S.K. Chanda, A.G. Schmidt, K. Godula, S.L. Leibel, J. Jose, K. D. Corbett, A.B. Ward, A.F. Carlin, J.D. Esko, SARS-CoV-2 infection depends on cellular heparan sulfate and ACE2, Cell 183 (4) (2020) 1043–1057 e15, https://doi.org/10.1016/j.cell.2020.09.033.
[51] P.S. Kwon, H. Oh, S.J. Kwon, W. Jin, F. Zhang, K. Fraser, J.J. Hong, R.J. Linhardt, J.S. Dordick, Sulfated polysaccharides effectively inhibit SARS-CoV-2 in vitro, Cell Discov. 6 (1) (2020) 50, https://doi.org/10.1038/s41421-020-00192-8.
[52] S.B. Kim, M. Zoepfl, P. Samanta, F. Zhang, K. Xia, R. Thara, R.J. Linhardt, R. J. Doerksen, M.A. McVoy, V.H. Pomin, Fractionation of sulfated galactan from the red alga Botryocladia occidentalis separates its anticoagulant and anti-SARS-CoV-2 properties, J. Biol. Chem. 298 (5) (2022), 101856, https://doi.org/10.1016/j.jbc.2022.101856.
[53] J. Lu, K.K. Shi, S. Chen, J. Wang, A. Hassouna, L.N. White, F. Merien, M. Xie, Q. Kong, J. Li, T. Ying, W.L. White, S. Nie, Fucoidan extracted from the New Zealand Undaria pinnatifida-physicochemical comparison against five other fucoidans: unique low molecular weight fraction bioactivity in breast cancer cell lines, Mar. Drugs 16 (12) (2018) 461, https://doi.org/10.3390/md16120461.
[54] L. Liu, X. Yang, P. Yuan, S. Cai, J. Bao, Y. Zhao, A. Aimaier, A. Aipire, J. Lu, J. Li, In vitro and in vivo dendritic cell immune stimulation effect of low molecular weight fucoidan from New Zealand Undaria pinnatifida, Mar. Drugs 20 (3) (2022) 197, https://doi.org/10.3390/md20030197.
[55] Y. Zhou, X. Chen, T. Chen, X. Chen, A review of the antibacterial activity and mechanisms of plant polysaccharides, Trends Food Sci. Technol. 123 (2022) 264–280, https://doi.org/10.1016/j.tifs.2022.03.020.
[56] O.N. Ayrapetyan, E.D. Obluchinskaya, E.V. Zhurishkina, Y.A. Skorik, D.V. Lebedev, A.A. Kulminskaya, I.M. Lapina, Antibacterial properties of fucoidans from the brown algae Fucus vesiculosus L. of the barents sea, Biology (Basel) 10 (1) (2021) 67, https://doi.org/10.3390/biology10010067.